doi:10.4149/neo_2018_180705N447

Development of a five-gene signature as a novel prognostic marker in ovarian cancer

R. WANG[1,#,*], X. H. YE[2,#], X. L. ZHAO[1], J. L. LIU[1], C. Y. ZHANG[1]

[1]Department of Gynecology and Obstetrics, Affiliated Heping Hospital of Changzhi Medical College, Changzhi Medical College, Changzhi 046000, China; [2]Department of Radiotherapy, First Affiliated Hospital of Zhejiang University School of Medicine, Zhejiang University School of Medicine, Hangzhou 310003, China

**Correspondence: Rwang_cz@aliyun.com*
#Contributed equally to this work.

Received July 5, 2018 / Accepted October 29, 2018

The prognosis of ovarian cancer (OC) remains poor. Thus, the present study aims to identify independent prognostic factor in OC patients. OC gene expression studies GSE26712 and TCGA-OV were included in this study. Prognosis-associated differentially expressed genes (DEGs) between normal ovarian tissue and OC were identified. LASSO Cox proportional hazards regression model was conducted and a prognostic signature was constructed based on these DEGs. The predictive ability of the signature was analyzed in the training set and test set. The prognosis performance of the signature was compared with CA-125 and HE4. Gene set enrichment analysis (GSEA) was conducted to identify relevant mechanism. 332 DEGs were identified, out of which 64 DEGs were significantly correlated with the overall survival (OS) of OC patients, and 5 DEGs (IGF2, PEG3, DCN, LYPD1 and RARRES1) were applied to build a 5-gene signature. Patients in the 5-gene signature low-risk group had significantly better OS compared to those in the 5-gene high-risk group (p=0.0004) in the training set. Similar results were found in the test set, and the signature was also an independent prognostic factor. The prognosis performance of the 5-gene signature was significantly better than that of CA-125 and HE4. GSEA suggested that OC samples in the 5-gene high-risk group were significantly enriched in WNT/β-catenin signaling and epithelial-mesenchymal transition. We developed and validated a 5-gene signature that might be used as an independent prognostic factor in patients with OS.

Key words: ovarian cancer; prognostic signature; overall survival

Ovarian cancer (OC) represents the most lethal type of gynecological malignance and is a clinically heterogeneous disease as demonstrated through associations with family history of cancer, genetic risk and histopathology of this disease [1, 2]. Epithelial cancer accounts for about 95% of the OC [2]. Owing to the fact that nearly 70% of OC patients are diagnosed at stages III and IV according to the International Federation of Gynecology and Obstetrics (FIGO) and that more than 30% of OC patients will develop acquired chemoresistance and eventually relapse, the 5-year overall survival remains poor [3, 4]. Thus, developing novel prognostic tools to stratify seemingly identical patients and redirect them to more precise therapies is of great importance. There have been many recent improvements in the sequencing technology. Subsequently, a variety of OC gene expression studies have been published [5, 6]. Therefore, in this study we developed and validated a five-gene based prognostic signature for patients with OC. It has been reported that these five genes (IGF2[7], PEG3[8], DCN[9], LYPD1[10] and RARRES1[11]) were associated with survival and cell growth of multiple human cancers.

Materials and methods

OC gene expression studies. OC gene expression study GSE26712 [5] and TCGA-OV [12] were included in this study. GSE26712, which included 195 ovary tissue samples (10 normal, 185 malignant) was used as a training set. TCGA-OV, which included 564 patients whose survival time was fully documented, was used as a test set.

Data processing and analysis. Raw data of GSE26712 was downloaded from gene expression omnibus (GEO)

database and preprocessed and normalized using R "affy" package [13], and then the DEGs between normal ovarian tissue and OC were calculated using R package "limma" [14]. Genes at $|\log_2 FC|>2$ and adjusted $p<0.05$ were treated as DEGs. Log-rank based survival analyses were conducted to identify DEGs that were significantly correlated with the overall survival (OS) of patients with OC. LASSO Cox regression model was applied to select prognostic DEGs to predict the OS by 10-fold cross-validation and the risk scores for each patient were calculated using R package "glmnet" [15]. Time-dependent receiver operating characteristic curve (ROC) analysis was conducted to find the optimal cut-off and stratify OC patients into low-risk group and high-risk group in the training set and test set [16]. Thus, we constructed a prognostic signature on the basis of LASSO Cox regression model. Logistic regression model and Cox proportional hazards regression model were performed to analyze the relation between the clinical features of OC patients and the 5-gene signature and to identify prognostic factors in OC. Odds ratios (ORs) or hazards ratios (HRs) and associated confidence intervals (CIs) were calculated using maximum likelihood estimates, along with Wald test

Table 1. Characteristics of OC patients in the test set.

Variable	total number	Group		Logistic regression analysis			
		Low-risk	High-risk	OR	LCI	UCI	p-value
Age (year)							
<60	295	112	183	1.002	0.987	1.017	0.783
≥60	269	107	162				
Stage							
Early stage	46	26	20	0.872	0.778	0.974	0.016
Late stage	518	193	325				
Grade							
Grade 1	9	7	2				
Grade 2	69	28	41	0.719	0.481	1.068	0.103
Grade 3	476	178	298				
NA	10	6	4				

Abbreviations: OR, odds ratio; LCI, lower limit of confidence interval; UCI, upper limit of confidence.

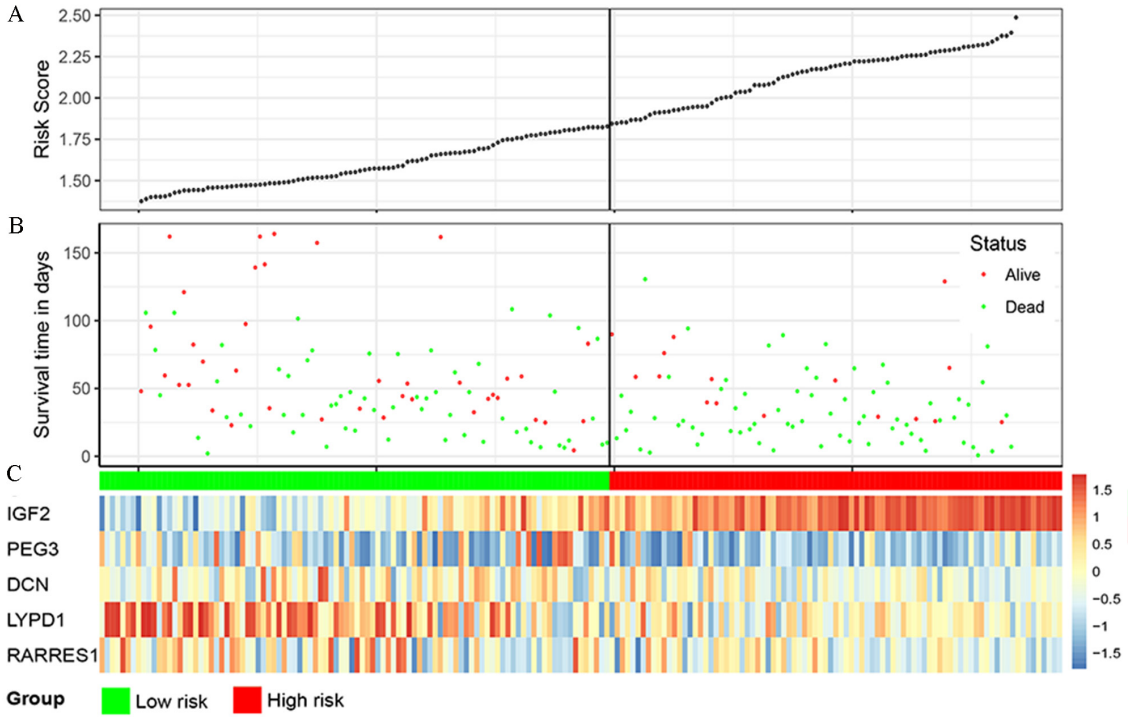

Figure 1. Characteristics of the 5-gene prognostic signature. A) the risk of each OC patients. B) the overall survival and survival status of each OC patients. C) heat-map of the 5 genes in the signature.

p-values. Thus, the prognostic role of the signature was investigated in the training set and test set. C-index, also known as concordance index, provides a global assessment of a fitted survival model. To evaluate the performance of the 5-gene signature, we compared the C-index of the 5-gene signature with other prognostic biomarkers (CA-125 and HE4) [17] using R package "survcomp [18]". Finally, to identify potentially relevant mechanisms that were associated with the OC patient survival, gene set enrichments analysis (GSEA) was conducted, and gene set at nominal p<0.05 and false discovery rate (FDR) <25% were treated as significantly enriched [19, 20].

Results

Characteristics of OC patients. A total of 185 high grade, advanced stage OC patients were included in the training set and the age of OC patients was not available. Meanwhile, a total of 564 OC patients were included in the TCGA-OV data set (the test set), of which 295 (52.3%) OC patients were younger than 60 years old and the remaining 269 OC patients were not younger than 60 years. Regarding the stage, 46 (8.2%) patients were early stage OC and 518 (91.8%) OC patients were advanced stage OC in the test set. As for the grade, 9 (1.6%) patients were grade 1 OC, 69 (12.2%) patients were grade 2 OC and 474 (84.4%) patients were grade 3 OC in the test set (Table 1).

Prognostic signature construction. As shown in Table S1, a total of 332 DEGs were identified between normal ovarian tissue and OC in the training set (Table S1). Then, 64 genes were significantly correlated with the OS of the OC patients using univariate Cox proportional hazards regression analysis (Table S2). We then constructed a 5-gene based prognostic signature using L1-penalized Cox proportional hazards regression on the training set (Figure 1, Table S3).

The prognostic role of the 5-gene signature in OC. We divided the OC patients into the 5-gene signature low-risk group and high-risk group on the basis of the cutoff (1.575) calculated using the time-dependent ROC analysis (Figure 2A). As shown in Figure 2B, patients in the 5-gene signature low-risk group had significantly better OS compared to those in the 5-gene high-risk group (HR= 0.5391, 95% CI: 0.3801–0.7646, p=0.0004).

Validation of the prognostic role of the 5-gene signature in the test set. To validate the predictive role of the 5-gene signature, we first performed logistic regression analysis. As shown in Table 1, the 5-gene signature was significantly correlated with the stage of OC patients (OR=0.872, 95% CI: 0.778–0.974, p=0.016, Table 1). The results of KM survival analysis suggest that the OS favors patients in 5-gene signature low-risk group over those in high-risk group (HR= 0.6186, 95% CI: 0.4849–0.7891, p=0.0001, Figure 3A) in the test set. Furthermore, although the 5-gene signature did not play a prognostic role in patients with early stage OC (HR= 0.4689, 95% CI: 0.1196–1.839, p=0.3, Figure 3B), a lower risk of signature was related with significantly better prognosis of patients with advanced stage OC (HR=0.6274, 95% CI: 0.4892–0.8047, p=0.0002, Figure 3C) in the set. Univariate and multivariable hazards regression analysis suggest that the 5-gene signature is an independent prognostic factor for OC (Table 2). Meanwhile, the results of Kaplan-Meier survival analysis suggest that lower expression of IGF2, DCN, LYPD1 and RARRES1 is associated with better OS in the training set and test set (Figure S1 and Figure S2).

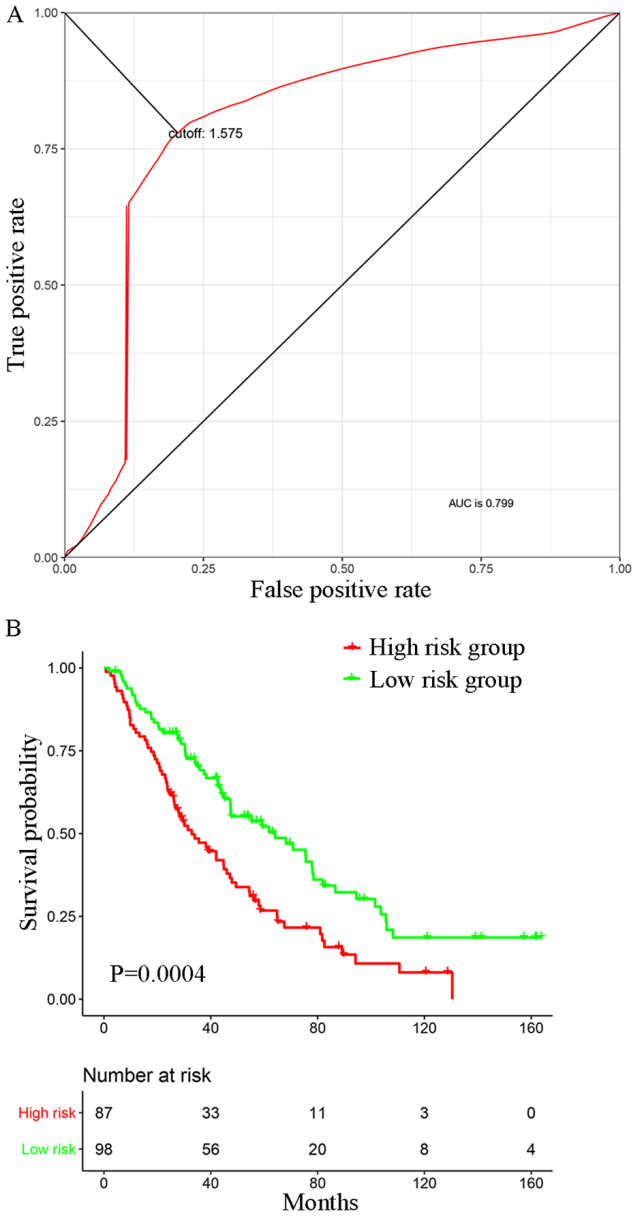

Figure 2. The prognostic role of the 5-gene signature in the training set. A) time-dependent survival ROC analysis. B) the overall survival of patients in low-risk group and high-risk group.

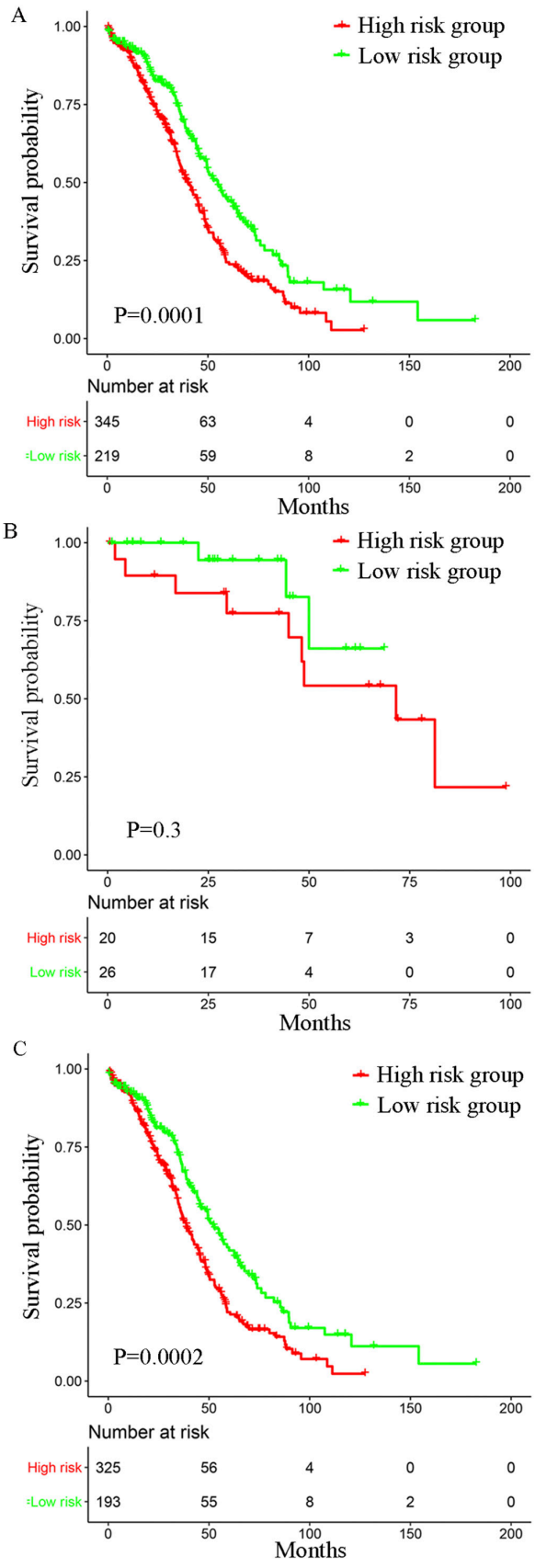

Figure 3. Validation of the prognostic role in the test set. A) the overall survival of patients in the whole population. B) the overall survival of patients with early stage OC. C) the overall survival of patients with advanced stage OC.

Comparison of the prognostic performance between the 5-gene signature and CA-125 and HE4. CA 125, also known as mucin 16 (MUC16), is a large membrane glycoprotein belonging to the wide mucin family and widely used as a tumor marker of OC [21]. Human epididymis protein 4 (HE4) is the FDC2 (HE4) gene product that has been treated as a new biomarker in OC[22]. Thus, we compared the prognosis performance of the 5-gene signature with CA-125 and HE4 in the TCGA ovarian cancer cohort (n=564). As shown in Figure 4, the C-index for the 5-gene signature is significantly higher compared to that for CA-125 (0.686 vs 0.539, p<0.001) and HE4 (0.686 vs 0.576, p<0.001) (Figure 4).

GSEA of OC samples. Finally, we conducted GSEA to find associated mechanisms confirming that the 5-gene signature affected the prognosis of patients with OC. As shown in Figure 5, OC samples in the 5-gene high-risk group were significantly enriched in WNT/β-catenin signaling (enrichment score: 0.514782, P: 0.024, FDR: 18.83%) and epithelial-mesenchymal transition (EMT) (enrichment score: 0.706814, p=0.0397, FDR: 5.07%).

Discussion

In this study, we identified DEGs between normal ovarian tissue and OC cells, identified prognostic DEGs correlated with the OS of OC patients, and a 5-gene signature was constructed after these prognostic DEGs were included into a Cox proportional hazards regression model combined with the least absolute shrinkage and selection operator. The prognostic role of the 5-gene signature was analyzed and validated in the training set and test set. Finally, GSEA was conducted to investigate potentially relevant mechanism.

Five genes in the prognostic signature were IGF2, PEG3, DCN, LYPD1 and RARRES1. In fact, there were several studies that have reported the 5 genes in the cancer pathogenesis and progression. Xu et al. suggested that the expression levels of IGF2 and CD133 were positively correlated with each other in primary ESCC [23] and that concurrent upregulation of IGF2 and CD133 expression was significantly related with poor patient prognosis. They were also found to be involved in colorectal cancer, liver cancer, adrenocortical carcinomas, etc. [7, 24, 25]. Meanwhile, Jiang et al. demonstrated that down-regulation of PEG3 stimulated beta-catenin pathway and promoted glioma cell growth, which was similar to the results of our GSEA showing that OC patients in the 5-gene high-risk group were significantly enriched in WNT/beta-catenin signaling pathway [26]. Li et al. demonstrated that DCN, accompanied by HSPD1, could be considered as a biomarker for colon cancer [27]. Xu Y et al. demonstrated that decreased expression of DCN promoted proliferation

Table 2. Univariate and multivariable Cox proportional hazards regression analysis on the overall survival of OC patients.

Variable	Univariate Cox proportional hazards regression analysis				Multivariable Cox proportional hazards regression analysis			
	HR	LCI	UCI	p-value	HR	LCI	UCI	p-value
Age	1.021	1.01	1.032	<0.001	1.021	1.011	1.032	<0.001
Stage	1.173	1.054	1.305	0.003	1.155	1.037	1.288	0.009
Grade	1.337	0.999	1.787	0.05	1.275	0.951	1.711	0.104
5-gene signature	3.484	1.187	10.23	0.023	3.842	1.289	11.459	0.016

Abbreviations: HR, hazards ratio; LCI, lower limit of confidence interval; UCI, upper limit of confidence interval.

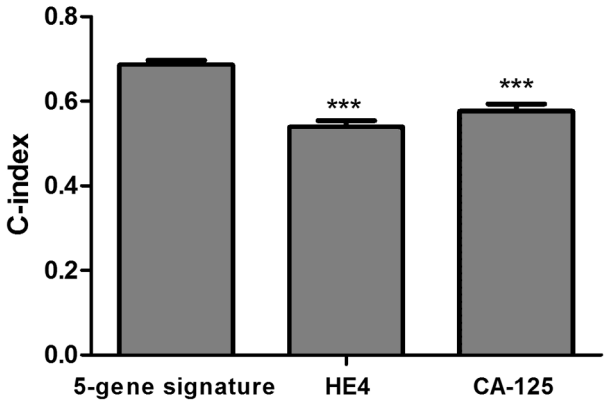

Figure 4. The C-index for the 5-gene signature, CA-125, and HE4. ***p<0.001

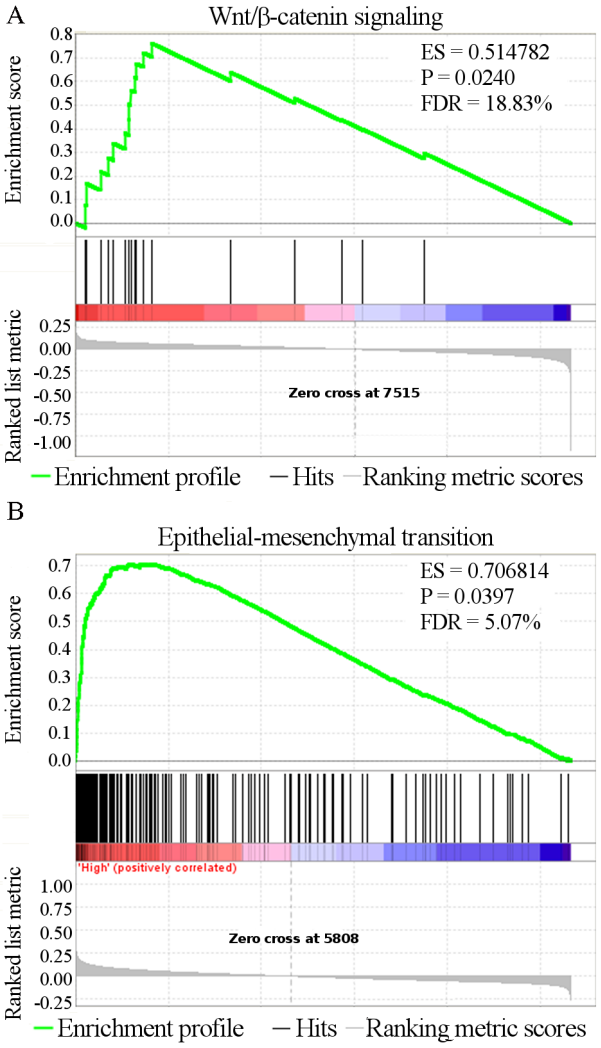

Figure 5. Gene set enrichment analysis of OC samples in the 5-gene signature low-risk group and high-risk group.

and metastasis of renal cell carcinoma cells [9]. Burnett et al. demonstrated that LYPD1 was up-regulated in breast cancer cells and was associated with the metastasis of the disease [28]. Oldridge et al. demonstrated that retinoic acid inhibited proliferation and invasion through inducting RARRES1 and LXN [29]. Wu et al. demonstrated that the expression of RARRES1 was significantly associated with tumor differentiation and staging in colorectal adenocarcinoma [11]. The above studies show that our signature might play an important role in the pathogenesis and progression of OC.

The result of GSEA suggest that the 5-gene signature might affect progression of the OC through WNT/β-catenin signaling and epithelial-mesenchymal transition. Wnt signaling was activated in epithelial OC and niclosamide inhibited the OC growth through suppressing WNT signaling. The Wnt signaling pathway plays a critical role in embryogenesis and oncogenesis. In the canonical Wnt signaling pathway, dysregulation of the Wnt/β-catenin signaling pathway has been identified in OC [30]. Mutations in the β-catenin (CTNNB1) gene leading to alteration of the Wnt/β-catenin signaling pathway have been found in the endometrioid subtype of OC [31, 32]. Aberrant accumulation of β-catenin is associated with increasing OC grade and poor survival [33, 34]. In contrast to canonical Wnt signaling, non-canonical Wnt signaling pathways may have transcriptional and non-transcriptional effects [34]. In the non-canonical Wnt/Ca2+ signaling pathway, Wnt ligands binding to Fzd receptors initiate activation of the phospholipase C via G protein-couple receptor signaling, causing an increase in intracellular Ca2+ and resulting in activation of Ca2+/calmodulin-dependent kinase II (CaMKII) and protein kinase C [35]. Meanwhile, previous studies have identified that deregulation of the Wnt/Ca2+ signaling pathway mediates cytoskeleton rearrangements, cellular

proliferation, cellular motility and epithelial-mesenchymal transition in cancer development and progression [36, 37].

Meanwhile, EMT has been found in multiple human cancers, especially in the metastasis process, where epithelial cells acquire increased motility and invasive properties to become mesenchymal like cells [38]. In OC, EMT promoted migration and invasion ability of the OC cells, contributed to chemoresistance and thus participated in the progression of the disease [39]. This could also explain the clinical role of the 5-gene signature in patients with OC to some extent.

Survival analysis on the 5-gene suggest that it could classify OC patients into high-risk group and low-risk group. Patients in low-risk group were associated with better clinical outcome compared with those in high-risk group. Although the conclusion was validated in an independent cohort, for the sake of caution we propose to conduct multicenter, large-scale clinical studies to validate our conclusions in the future.

In conclusion, we developed a 5-gene signature that might be used as an independent prognostic factor in patients with OC.

Supplementary information is available in the online version of the paper.

Acknowledgments: This work was supported by Zhejiang Province Science Technology Foundation (No. 2015C33199).

References

[1] HALKIA E, CHRELIAS G, CHRELIAS C, ESQUIVEL J. 2017 Update on Ovarian Cancer Peritoneal Carcinomatosis Multimodal-Treatment Considerations. Gastroenterol Res Pract 2018; 2018: 5284814. https://doi.org/10.1155/2018/5284814

[2] ABDULFATAH E, AHMED Q, ALOSH B, BANDYOPADHYAY S, BLUTH MH et al. Gynecologic Cancers: Molecular Updates 2018. Clin Lab Med 2018; 38: 421–438. https://doi.org/10.1016/j.cll.2018.02.007

[3] TYAGI NK, DHESY-THIND S. Clinical practice guidelines in breast cancer. Curr Oncol 2018; 25: S151–S160. https://doi.org/10.3747/co.25.3729

[4] HENDERSON JT, WEBBER EM, SAWAYA GF. Screening for Ovarian Cancer: Updated Evidence Report and Systematic Review for the US Preventive Services Task Force. JAMA 2018; 319: 595–606. https://doi.org/10.1001/jama.2017.21421

[5] BONOME T, LEVINE DA, SHIH J, RANDONOVICH M, PISE-MASISON CA et al: A gene signature predicting for survival in suboptimally debulked patients with ovarian cancer. Cancer Res 2008; 68: 5478–5486. https://doi.org/10.1158/0008-5472.CAN-07-6595

[6] MOK SC, BONOME T, VATHIPADIEKAL V, BELL A, JOHNSON ME et al: A gene signature predictive for outcome in advanced ovarian cancer identifies a survival factor: microfibril-associated glycoprotein 2. Cancer Cell 2009; 16: 521–532. https://doi.org/10.1016/j.ccr.2009.10.018

[7] THOMAS H. Liver cancer: IGF2 – an epigenetic oncodriver in HCC. Nat Rev Gastroenterol Hepatol 2016; 13: 625. https://doi.org/10.1038/nrgastro.2016.162

[8] NYE MD, HOYO C, HUANG Z, VIDAL AC, WANG F et al: Associations between methylation of paternally expressed gene 3 (PEG3), cervical intraepithelial neoplasia and invasive cervical cancer. PLoS One 2013; 8: e56325. https://doi.org/10.1371/journal.pone.0056325

[9] XU Y, XIA Q, RAO Q, SHI S, SHI Q et al. DCN deficiency promotes renal cell carcinoma growth and metastasis through downregulation of P21 and E-cadherin. Tumour Biol 2016; 37: 5171–5183. https://doi.org/10.1007/s13277-015-4160-1

[10] YU DH, FAN W, LIU G, NGUY V, CHATTERTON JE et al: PHTS, a novel putative tumor suppressor, is involved in the transformation reversion of HeLaHF cells independently of the p53 pathway. Exp Cell Res 2006; 312: 865–876. https://doi.org/10.1016/j.yexcr.2005.12.006

[11] WU CC, SHYU RY, CHOU JM, JAO SW, CHAO PC et al. RARRES1 expression is significantly related to tumour differentiation and staging in colorectal adenocarcinoma. Eur J Cancer 2006; 42: 557–565. https://doi.org/10.1016/j.ejca.2005.11.015

[12] CANCER GENOME ATLAS RESEARCH NETWORK. Integrated genomic analyses of ovarian carcinoma. Nature 2011; 474: 609–615. https://doi.org/10.1038/nature10166

[13] GAUTIER L, COPE L, BOLSTAD BM, IRIZARRY RA. affy-analysis of Affymetrix GeneChip data at the probe level. Bioinformatics 2004; 20: 307–315. https://doi.org/10.1093/bioinformatics/btg405

[14] RITCHIE ME, PHIPSON B, WU D, HU Y, LAW CW et al. limma powers differential expression analyses for RNA-sequencing and microarray studies. Nucleic Acids Res 2015; 43: e47. https://doi.org/10.1093/nar/gkv007

[15] FRIEDMAN J, HASTIE T, TIBSHIRANI R. Regularization Paths for Generalized Linear Models via Coordinate Descent. J Stat Softw 2010; 33: 1–22.

[16] HEAGERTY PJ, LUMLEY T, PEPE MS. Time-dependent ROC curves for censored survival data and a diagnostic marker. Biometrics 2000; 56: 337–344.

[17] STEFFENSEN KD, WALDSTROM M, BRANDSLUND I, PETZOLD M, JAKOBSEN A. The prognostic and predictive value of combined HE4 and CA-125 in ovarian cancer patients. Int J Gynecol Cancer 2012; 22: 1474–1482. https://doi.org/10.1097/IGC.0b013e3182681cfd

[18] SCHRODER MS, CULHANE AC, QUACKENBUSH J, HAIBE-KAINS B. survcomp: an R/Bioconductor package for performance assessment and comparison of survival models. Bioinformatics 2011; 27: 3206–3208. https://doi.org/10.1093/bioinformatics/btr511

[19] SUBRAMANIAN A, TAMAYO P, MOOTHA VK, MUKHERJEE S, EBERT BL et al: Gene set enrichment analysis: a knowledge-based approach for interpreting genome-wide expression profiles. Proc Natl Acad Sci U S A 2005; 102: 15545–15550. https://doi.org/10.1073/pnas.0506580102

[20] MOOTHA VK, LINDGREN CM, ERIKSSON KF, SUBRAMANIAN A, SIHAG S et al: PGC-1alpha-responsive genes involved in oxidative phosphorylation are coordinately downregulated in human diabetes. Nat Genet 2003; 34: 267–273. https://doi.org/10.1038/ng1180

[21] BOTTONI P, SCATENA R. The Role of CA 125 as Tumor Marker: Biochemical and Clinical Aspects. Adv Exp Med Biol 2015; 867: 229–244. https://doi.org/10.1007/978-94-017-7215-0_14

[22] SIMMONS AR, BAGGERLY K, BAST RC JR. The emerging role of HE4 in the evaluation of epithelial ovarian and endometrial carcinomas. Oncology (Williston Park) 2013; 27: 548–556.

[23] XU WW, LI B, ZHAO JF, YANG JG, LI JQ et al. IGF2 induces CD133 expression in esophageal cancer cells to promote cancer stemness. Cancer Lett 2018; 425: 88–100. https://doi.org/10.1016/j.canlet.2018.03.039

[24] CUI H, LIU Y, JIANG J, LIU Y, YANG Z et al. IGF2-derived miR-483 mediated oncofunction by suppressing DLC-1 and associated with colorectal cancer. Oncotarget 2016; 7: 48456–48466. https://doi.org/10.18632/oncotarget.10309

[25] CREEMERS SG, VAN KOETSVELD PM, VAN KEMENADE FJ, PAPATHOMAS TG, FRANSSEN GJ et al: Methylation of IGF2 regulatory regions to diagnose adrenocortical carcinomas. Endocr Relat Cancer 2016; 23: 727–737. https://doi.org/10.1530/ERC-16-0266

[26] JIANG X, YU Y, YANG HW, AGAR NY, FRADO L et al. The imprinted gene PEG3 inhibits Wnt signaling and regulates glioma growth. J Biol Chem 2010; 285: 8472–8480. https://doi.org/10.1074/jbc.M109.069450

[27] LI G, LI M, LIANG X, XIAO Z, ZHANG P et al. Identifying DCN and HSPD1 as Potential Biomarkers in Colon Cancer Using 2D-LC-MS/MS Combined with iTRAQ Technology. J Cancer 2017; 8: 479–489. https://doi.org/10.7150/jca.17192

[28] BURNETT RM, CRAVEN KE, KRISHNAMURTHY P, GOSWAMI CP, BADVE S et al. Organ-specific adaptive signaling pathway activation in metastatic breast cancer cells. Oncotarget 2015; 6: 12682–12696. https://doi.org/10.18632/oncotarget.3707

[29] OLDRIDGE EE, WALKER HF, STOWER MJ, SIMMS MS, MANN VM et al. Retinoic acid represses invasion and stem cell phenotype by induction of the metastasis suppressors RARRES1 and LXN. Oncogenesis 2013; 2: e45. https://doi.org/10.1038/oncsis.2013.6

[30] ZHAO H, WEI W, SUN Y, GAO J, WANG Q et al. Interference with the expression of beta-catenin reverses cisplatin resistance in A2780/DDP cells and inhibits the progression of ovarian cancer in mouse model. DNA Cell Biol 2015; 34: 55–62. https://doi.org/10.1089/dna.2014.2626

[31] BARGHOUT SH, ZEPEDA N, XU Z, STEED H, LEE CH et al. Elevated beta-catenin activity contributes to carboplatin resistance in A2780cp ovarian cancer cells. Biochem Biophys Res Commun 2015; 468: 173–178. https://doi.org/10.1016/j.bbrc.2015.10.138

[32] AREND RC, LONDONO-JOSHI AI, STRAUGHN JM, JR., BUCHSBAUM DJ. The Wnt/beta-catenin pathway in ovarian cancer: a review. Gynecol Oncol 2013; 131: 772–779. https://doi.org/10.1016/j.ygyno.2013.09.034

[33] MCCONECHY MK, DING J, SENZ J, YANG W, MELNYK N et al: Ovarian and endometrial endometrioid carcinomas have distinct CTNNB1 and PTEN mutation profiles. Mod Pathol 2014; 27: 128–134. https://doi.org/10.1038/modpathol.2013.107

[34] FORD CE, PUNNIA-MOORTHY G, HENRY CE, LLAMOSAS E, NIXDORF S et al. The non-canonical Wnt ligand, Wnt5a, is upregulated and associated with epithelial to mesenchymal transition in epithelial ovarian cancer. Gynecol Oncol 2014; 134: 338–345. https://doi.org/10.1016/j.ygyno.2014.06.004

[35] LIU LJ, XIE SX, CHEN YT, XUE JL, ZHANG CJ et al. Aberrant regulation of Wnt signaling in hepatocellular carcinoma. World J Gastroenterol 2016; 22: 7486–7499. https://doi.org/10.3748/wjg.v22.i33.7486

[36] HUANG L, JIN Y, FENG S, ZOU Y, XU S et al. Role of Wnt/beta-catenin, Wnt/c-Jun N-terminal kinase and Wnt/Ca(2+) pathways in cisplatin-induced chemoresistance in ovarian cancer. Exp Ther Med 2016; 12: 3851–3858. https://doi.org/10.3892/etm.2016.3885

[37] GREGORY MA, PHANG TL, NEVIANI P, ALVAREZ-CALDERON F, EIDE CA et al. Wnt/Ca2+/NFAT signaling maintains survival of Ph+ leukemia cells upon inhibition of Bcr-Abl. Cancer Cell 2010; 18: 74–87. https://doi.org/10.1016/j.ccr.2010.04.025

[38] YO YT, LIN YW, WANG YC, BALCH C, HUANG RL et al. Growth inhibition of ovarian tumor-initiating cells by niclosamide. Mol Cancer Ther 2012; 11: 1703–1712. https://doi.org/10.1158/1535-7163.MCT-12-0002

[39] JEON SY, HWANG KA, CHOI KC. Effect of steroid hormones, estrogen and progesterone, on epithelial mesenchymal transition in ovarian cancer development. J Steroid Biochem Mol Biol 2016; 158: 1–8. https://doi.org/10.1016/j.jsbmb.2016.02.005

Development of a five-gene signature as a novel prognostic marker in ovarian cancer

R. WANG[1,#,*], X. H. YE[2,#], X. L. ZHAO[1], J. L. LIU[1], C. Y. ZHANG[1]

Supplemental material

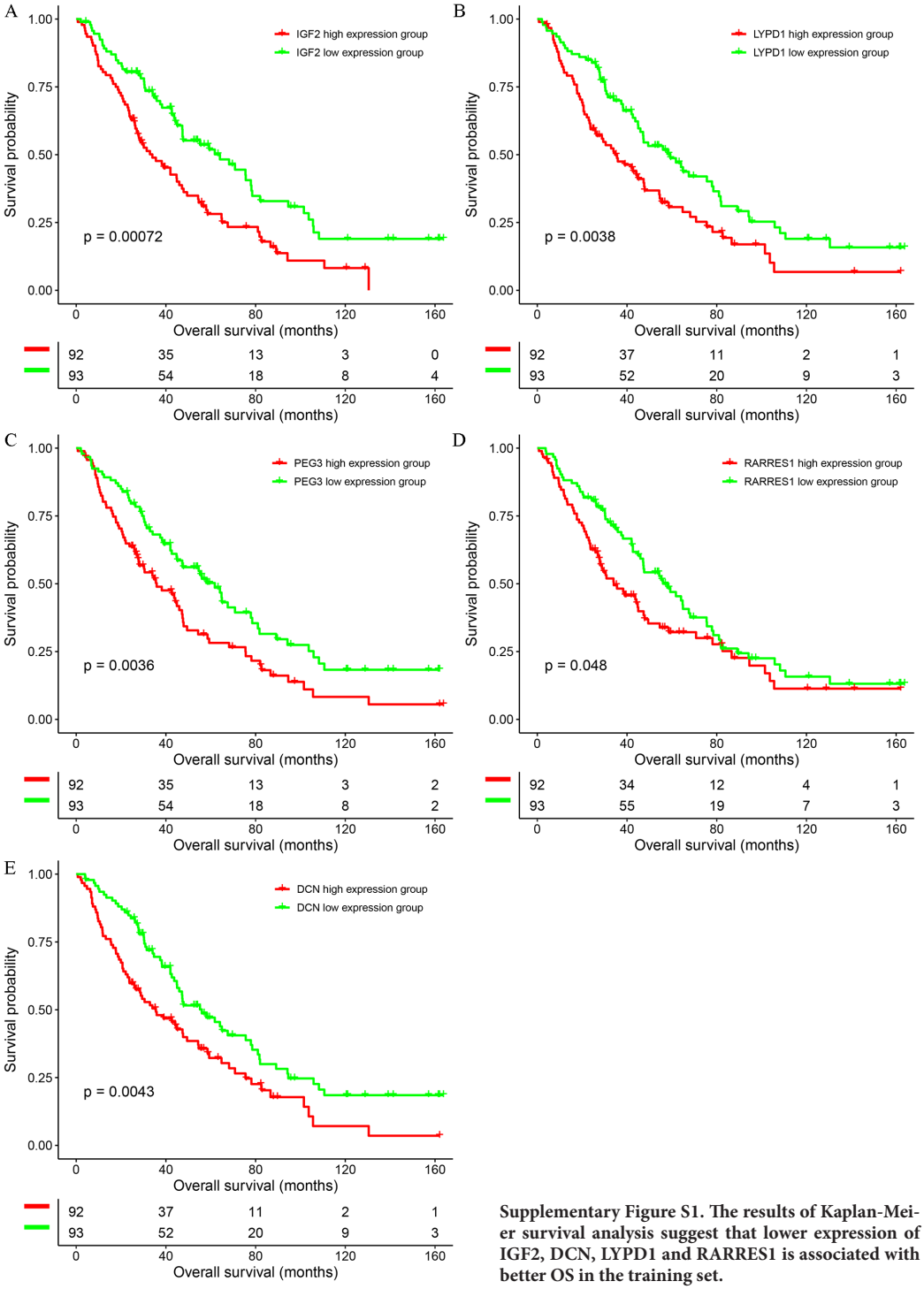

Supplementary Figure S1. The results of Kaplan-Meier survival analysis suggest that lower expression of IGF2, DCN, LYPD1 and RARRES1 is associated with better OS in the training set.

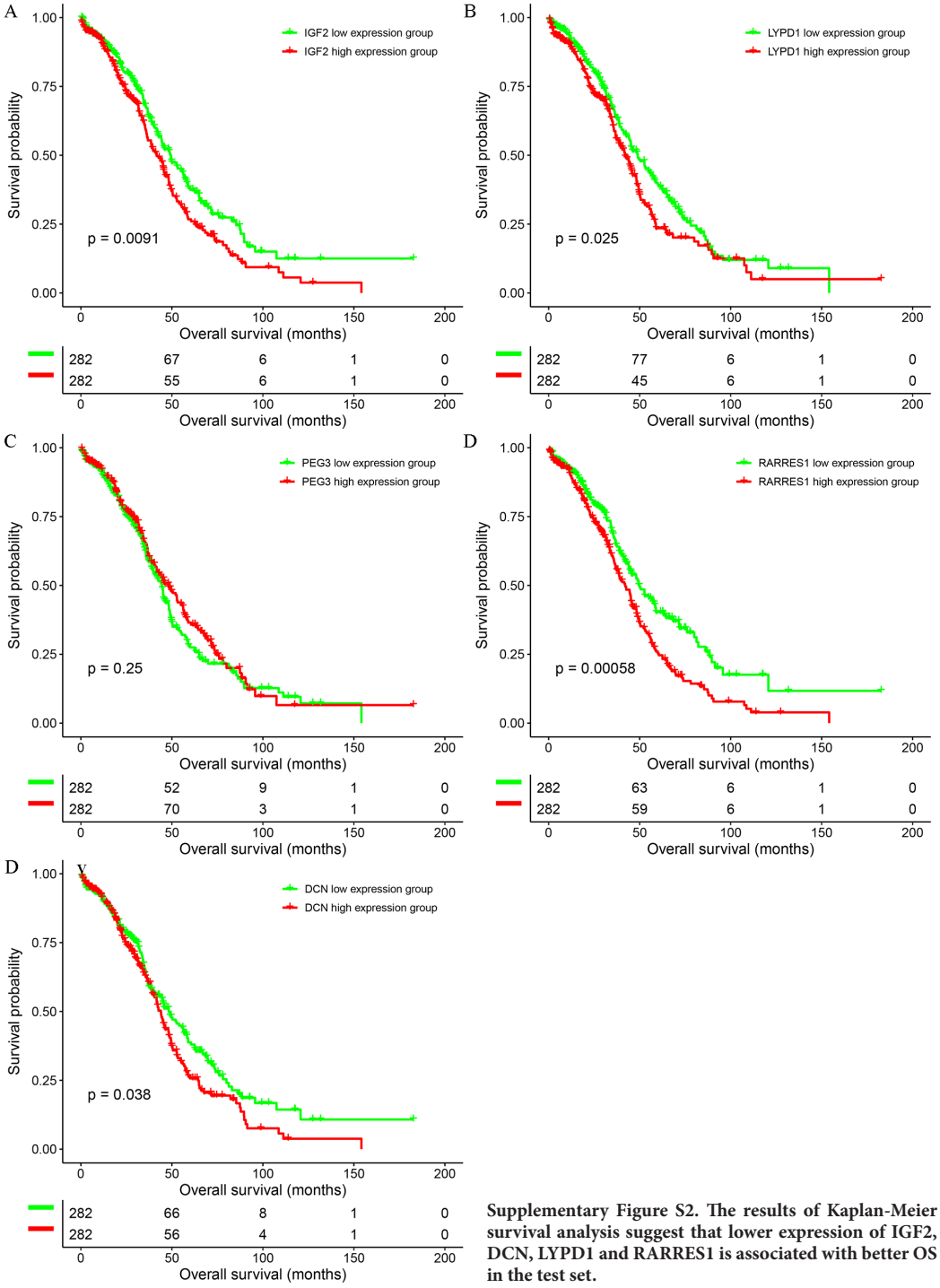

Supplementary Figure S2. The results of Kaplan-Meier survival analysis suggest that lower expression of IGF2, DCN, LYPD1 and RARRES1 is associated with better OS in the test set.

Supplementary Table 1. 332 differentially expressed gene between normal ovary tissue and OC.

Probe ID	Adjusted p-value	logFC	Gene symbol
204719_at	2.22E-19	−4.16776	ABCA8
201963_at	2.52E-10	−2.25638	ACSL1
X00351_5_at	8.42E-07	2.660791	ACTB
202381_at	1.46E-12	−2.26269	ADAM9
214913_at	4.12E-20	−2.13792	ADAMTS3
212070_at	5.27E-09	2.229783	ADGRG1
213094_at	2.96E-14	−2.04628	ADGRG6
209613_s_at	2.09E-11	−3.66243	ADH1B
208848_at	7.89E-11	−2.06097	ADH5
212224_at	2.09E-12	−2.77912	ALDH1A1
222108_at	2.01E-14	−2.79646	AMIGO2
206385_s_at	2.08E-11	−2.0723	ANK3
205206_at	6.39E-14	−2.19893	ANOS1
209369_at	1.83E-13	−2.80928	ANXA3
203074_at	1.10E-42	−3.40031	ANXA8L1
205083_at	5.21E-34	−4.22561	AOX1
205568_at	1.04E-29	−2.72917	AQP9
213618_at	1.25E-26	−2.207	ARAP2
205414_s_at	3.48E-35	−2.23218	ARHGAP44
206167_s_at	3.13E-20	−2.24395	ARHGAP6
218694_at	8.93E-30	−3.45138	ARMCX1
222103_at	1.04E-13	−2.04397	ATF1
201855_s_at	2.78E-22	−2.09125	ATMIN
213238_at	3.75E-38	−2.27162	ATP10D
209186_at	8.59E-10	2.002041	ATP2A2
210149_s_at	2.87E-14	2.303593	ATP5H
213106_at	1.13E-34	−2.32718	ATP8A1
203232_s_at	1.74E-18	−2.34824	ATXN1
203304_at	3.14E-11	−2.0492	BAMBI
203009_at	7.69E-10	2.000145	BCAM
205433_at	3.32E-32	−4.43005	BCHE
201545_s_at	1.19E-17	2.187724	PABPN1
213429_at	1.44E-18	−2.1286	BICC1
206581_at	3.33E-79	−3.72993	BNC1
209430_at	7.98E-31	−2.74434	BTAF1
219010_at	1.52E-11	2.059427	C1orf106
220543_at	9.76E-40	−2.11256	C21orf62
204480_s_at	6.63E-25	2.809954	C9orf16
205428_s_at	9.23E-39	−3.89844	CALB2
200935_at	2.71E-13	2.3752	CALR
212586_at	9.33E-15	−2.48788	CAST
212097_at	3.15E-11	−2.86996	CAV1
203324_s_at	1.07E-11	−2.07008	CAV2
216379_x_at	3.06E-20	4.345562	CD24
202870_s_at	9.16E-08	2.068895	CDC20
202156_s_at	1.76E-23	−2.1972	CELF2
213800_at	4.63E-10	−2.26546	CFH
215388_s_at	9.63E-11	−2.35194	CFHR1
203854_at	3.66E-14	−2.58878	CFI
204260_at	7.66E-25	−2.07391	CHGB
202536_at	4.04E-12	−2.0542	CHMP2B
218085_at	8.37E-11	−2.0057	CHMP5
209763_at	9.74E-23	−3.61456	CHRDL1
200810_s_at	1.48E-11	−2.16049	CIRBP
204170_s_at	4.29E-07	2.362744	CKS2
219640_at	1.21E-46	−2.25056	CLDN15
203953_s_at	2.38E-12	3.892081	CLDN3
201428_at	4.48E-12	2.101791	CLDN4
207995_s_at	5.18E-45	−2.51265	CLEC4M
213317_at	6.69E-08	−2.60302	CLIC5
214683_s_at	3.62E-20	−2.18401	CLK1
202310_s_at	2.05E-07	3.226624	COL1A1
209156_s_at	5.35E-04	2.131939	COL6A2
202110_at	2.24E-09	2.04221	COX7B
204846_at	7.34E-08	2.329078	CP
201116_s_at	1.30E-12	−2.04869	CPE
208146_s_at	1.81E-13	−2.4312	CPVL
202575_at	9.49E-14	3.312046	CRABP2
201989_s_at	8.59E-33	−2.42911	CREBL2
219049_at	8.42E-17	−2.31946	CSGALNACT1
215121_x_at	1.51E-03	2.203539	CYAT1
203139_at	1.62E-21	−2.24884	DAPK1
209335_at	3.32E-05	−2.15118	DCN
212855_at	4.17E-36	−2.02338	DCUN1D4
213998_s_at	2.24E-18	−2.88849	DDX17
210397_at	1.53E-04	2.541294	DEFB1
203695_s_at	3.11E-43	−3.34069	DFNA5
215506_s_at	7.70E-16	−2.77867	DIRAS3
201681_s_at	4.79E-12	−2.02762	DLG5
203881_s_at	2.03E-17	−2.62651	DMD
205003_at	2.94E-12	−2.36394	DOCK4
204646_at	4.17E-27	−3.72056	DPYD
200762_at	4.68E-12	−2.54164	DPYSL2
206032_at	2.22E-38	−2.26127	DSC3
218854_at	1.09E-21	−3.07949	DSE
206101_at	7.51E-18	−2.56347	ECM2
201843_s_at	6.58E-24	−3.89742	EFEMP1
219833_s_at	7.12E-18	−2.08989	EFHC1
210827_s_at	3.69E-13	2.621677	ELF3
217294_s_at	3.83E-04	2.044274	ENO1
217886_at	9.18E-25	−2.03626	EPS15
217234_s_at	4.96E-17	−2.01056	EZR
218518_at	3.42E-24	−2.76031	FAM13B
215000_s_at	4.12E-20	−2.38943	FEZ2
205110_s_at	4.69E-37	−2.75939	FGF13
206404_at	6.00E-13	−2.4197	FGF9
219250_s_at	3.70E-13	−2.26279	FLRT3
204437_s_at	1.83E-11	3.4742	FOLR1
213056_at	1.17E-25	−2.72701	FRMD4B
204072_s_at	6.93E-34	−3.10251	FRY
202489_s_at	2.68E-07	2.127299	FXYD3
203706_s_at	1.38E-10	−2.23584	FZD7
211458_s_at	4.47E-10	−2.26778	GABARAPL3
204417_at	1.68E-20	−2.33445	GALC
218885_s_at	9.83E-24	−2.1412	GALNT12
204457_s_at	6.78E-11	−2.7071	GAS1

Supplementary Table 1. ***Continued***

Probe ID	Adjusted p-value	logFC	Gene symbol
210002_at	4.53E-10	–2.86424	GATA6
203765_at	3.77E-19	–2.33892	GCA
212244_at	3.76E-32	–2.32237	GCOM1
205100_at	2.23E-23	–2.24551	GFPT2
205498_at	7.36E-18	–2.52147	GHR
201667_at	1.22E-04	–2.04991	GJA1
203159_at	6.62E-28	–2.09898	GLS
204115_at	3.97E-10	–2.14425	GNG11
209469_at	2.01E-62	–3.85864	GPM6A
204137_at	7.44E-20	–2.15283	GPR137B
204793_at	1.56E-14	–2.31537	GPRASP1
205862_at	2.10E-15	–2.69417	GREB1
212090_at	2.01E-16	2.174916	GRINA
222150_s_at	1.77E-26	–2.40013	GSAP
200824_at	3.94E-20	2.442904	GSTP1
205436_s_at	5.25E-15	2.294294	H2AFX
208579_x_at	1.40E-09	2.404874	H2BFS
207316_at	3.81E-15	–2.02722	HAS1
214414_x_at	1.50E-07	–3.57167	HBA2
209116_x_at	4.03E-08	–4.09804	HBB
213515_x_at	8.43E-20	–2.45235	HBG2
213069_at	7.70E-22	–3.1479	HEG1
209398_at	3.51E-06	2.025838	HIST1H1C
214290_s_at	9.29E-17	3.813299	HIST2H2AA4
206074_s_at	1.15E-13	2.469522	HMGA1
221480_at	2.23E-57	–2.14345	HNRNPD
206858_s_at	5.97E-19	–2.64051	HOXC6
206697_s_at	1.24E-06	–2.75649	HP
208470_s_at	5.52E-05	–2.18991	HPR
217989_at	3.76E-11	–2.02168	HSD17B11
201655_s_at	1.79E-12	2.096271	HSPG2
209292_at	1.74E-10	–2.82513	ID4
210046_s_at	8.51E-10	2.058312	IDH2
202411_at	1.39E-04	2.038914	IFI27
204415_at	8.26E-06	2.053799	IFI6
202718_at	3.15E-15	3.881271	IGFBP2
203851_at	2.67E-11	–2.28862	IGFBP6
217022_s_at	3.87E-03	2.3252	IGHA2
214677_x_at	5.70E-03	2.574819	IGLC1
215379_x_at	3.50E-03	2.064311	IGLV1-44
212195_at	1.03E-09	–2.74261	IL6ST
202409_at	3.42E-03	2.47873	IGF2
205483_s_at	9.44E-07	2.450106	ISG15
218170_at	3.77E-15	–2.15637	ISOC1
205786_s_at	2.57E-23	–2.26522	ITGAM
201473_at	6.57E-08	2.126389	JUNB
203845_at	6.05E-20	–2.11657	KAT2B
200922_at	1.46E-12	2.028977	KDELR1
203934_at	1.16E-72	–3.11676	KDR
221841_s_at	7.46E-06	–2.22342	KLF4
204733_at	2.69E-08	2.560931	KLK6
206125_s_at	1.41E-09	2.031964	KLK8
202202_s_at	4.57E-17	–2.71428	LAMA4
201505_at	3.82E-09	–2.23483	LAMB1
212531_at	4.83E-06	2.597947	LCN2
208450_at	1.10E-22	–2.19929	LGALS2
208933_s_at	4.13E-36	–3.35962	LGALS8
206140_at	1.32E-40	–3.75029	LHX2
201847_at	1.47E-08	–2.0862	LIPA
200772_x_at	7.63E-16	2.162312	PTMA
204359_at	5.87E-22	–4.00834	FLRT2
201278_at	5.57E-28	–2.89922	DAB2
207016_s_at	1.02E-32	–4.36511	ALDH1A2
222281_s_at	1.99E-12	3.880707	C1orf186
202551_s_at	7.80E-12	–2.11329	CRIM1
214945_at	1.16E-54	–4.66198	LOC101930363
202736_s_at	3.45E-08	2.220243	LSM4
208835_s_at	6.66E-10	–2.23185	LUC7L3
218729_at	2.14E-11	–2.48403	LXN
212909_at	2.41E-05	2.098813	LYPD1
209348_s_at	2.63E-30	–3.18447	MAF
205027_s_at	1.02E-32	–2.15682	MAP3K8
205819_at	5.91E-22	–2.70494	MARCO
209035_at	3.04E-06	2.026546	MDK
204059_s_at	5.74E-31	–2.27797	ME1
221884_at	7.17E-14	2.87032	MECOM
209200_at	2.34E-15	–2.01228	MEF2C
207480_s_at	2.50E-22	–3.05219	MEIS2
203510_at	6.90E-22	–3.20603	MET
207761_s_at	1.21E-12	–2.55681	METTL7A
217756_x_at	1.04E-17	2.010399	SERF2
214696_at	1.07E-15	–2.36434	MIR22HG
203189_s_at	2.81E-12	2.195696	NDUFS8
211430_s_at	1.29E-02	2.369659	IGHG1
203878_s_at	2.79E-06	2.216431	MMP11
204259_at	3.57E-04	2.159356	MMP7
204959_at	5.44E-55	–4.43974	MNDA
204331_s_at	4.64E-06	2.088749	MRPS12
212096_s_at	5.40E-19	–2.46268	MTUS1
213693_s_at	8.79E-10	2.910366	MUC1
221899_at	5.72E-17	–2.8265	N4BP2L2
204749_at	1.43E-30	–3.28136	NAP1L3
33767_at	3.74E-11	–2.06774	NEFH
203413_at	6.56E-61	–3.68444	NELL2
209706_at	5.86E-48	–2.57723	NKX3-1
203238_s_at	7.72E-20	2.764711	NOTCH3
205440_s_at	6.13E-54	–3.67194	NPY1R
209505_at	2.25E-13	–2.69013	NR2F1
209120_at	1.31E-06	–2.05081	NR2F2
209570_s_at	9.15E-14	–2.55553	NSG1
222203_s_at	8.05E-25	–2.16961	RDH14
218051_s_at	5.54E-10	2.135175	NT5DC2
218730_s_at	1.46E-15	–2.36917	OGN
217525_at	2.94E-22	–2.44233	OLFML1
209552_at	2.55E-11	2.121913	PAX8
218515_at	9.15E-25	–2.0084	PAXBP1

Supplementary Table 1. ***Continued***

Probe ID	Adjusted p-value	logFC	Gene symbol
219737_s_at	4.26E-35	−2.20263	PCDH9
219295_s_at	1.16E-22	−2.22582	PCOLCE2
213228_at	1.14E-36	−2.39896	PDE8B
218718_at	9.41E-12	−2.39503	PDGFC
219304_s_at	2.64E-20	−2.99789	PDGFD
221898_at	5.78E-22	−2.14319	PDPN
209493_at	1.16E-12	−2.04241	PDZD2
200787_s_at	8.52E-15	2.252569	PEA15
209242_at	1.54E-06	−3.1553	PEG3
200634_at	9.36E-20	3.398226	PFN1
213227_at	1.32E-21	−2.26637	PGRMC2
204049_s_at	6.51E-27	−2.42175	PHACTR2
203688_at	1.14E-15	−2.20414	PKD2
201251_at	1.99E-19	3.262371	PKM
213222_at	4.75E-10	−2.05202	PLCB1
205111_s_at	4.88E-39	−2.22766	PLCE1
209122_at	3.42E-09	−2.01881	PLIN2
210946_at	2.25E-24	−2.90344	PLPP1
218901_at	6.27E-26	−3.39253	PLSCR4
212179_at	2.09E-20	−2.42237	PNISR
217779_s_at	1.24E-18	−2.03972	PNRC2
201578_at	9.28E-11	−2.18479	PODXL
218010_x_at	2.74E-24	2.918798	PPDPF
212215_at	2.59E-21	−2.16514	PREPL
206007_at	9.61E-47	−2.95447	PRG4
200603_at	1.50E-12	−2.24346	PRKAR1A
203680_at	1.92E-11	−2.13829	PRKAR2B
200707_at	3.24E-11	2.19688	PRKCSH
206445_s_at	1.00E-16	2.226572	PRMT1
201300_s_at	8.02E-08	−2.0224	PRNP
203650_at	5.92E-41	−3.47704	PROCR
207808_s_at	4.22E-22	−3.3456	PROS1
202525_at	1.07E-09	2.003049	PRSS8
203355_s_at	1.95E-52	−3.31581	PSD3
213933_at	7.43E-20	−2.30298	PTGER3
204897_at	3.90E-15	−2.68542	PTGER4
208131_s_at	6.30E-09	−2.60326	PTGIS
212588_at	1.55E-10	−2.16582	PTPRC
204020_at	5.67E-14	−2.09451	PURA
212636_at	1.35E-16	−2.5737	QKI
218668_s_at	1.48E-20	−2.29864	RAP2C
221872_at	3.42E-06	−2.62375	RARRES1
212027_at	9.36E-14	−2.29353	RBM25
205407_at	1.08E-22	−2.3872	RECK
204364_s_at	2.61E-53	−3.94761	REEP1
204337_at	1.56E-16	−2.86813	RGS4
212099_at	1.88E-09	2.6548	RHOB
218323_at	3.42E-25	−2.08571	RHOT1
213397_x_at	5.32E-16	−2.92585	RNASE4
214041_x_at	1.19E-21	3.167255	RPL37A
200082_s_at	4.05E-18	3.064104	RPS7
209006_s_at	8.53E-27	−2.77715	RSRP1
203485_at	1.85E-30	−2.94876	RTN1

Probe ID	Adjusted p-value	logFC	Gene symbol
200660_at	1.99E-11	2.556766	S100A11
202598_at	9.60E-17	2.6354	S100A13
204268_at	2.21E-06	2.405757	S100A2
217728_at	5.21E-11	2.222818	S100A6
218370_s_at	4.87E-44	−2.25463	S100PBP
200847_s_at	1.83E-13	−2.38721	SARAF
203889_at	2.03E-11	−2.75873	SCG5
205979_at	1.76E-06	3.591818	SCGB2A1
201339_s_at	1.72E-07	−2.01388	SCP2
212314_at	2.82E-16	−2.15107	SEL1L3
203789_s_at	2.41E-09	−2.5231	SEMA3C
213169_at	2.26E-25	−2.26337	SEMA5A
209723_at	1.05E-16	−2.13449	SERPINB9
215780_s_at	4.75E-09	2.208081	SET
202037_s_at	4.56E-16	−3.1809	SFRP1
202234_s_at	4.57E-24	−2.55208	SLC16A1
219215_s_at	1.65E-09	2.042175	SLC39A4
209267_s_at	2.39E-23	−3.62037	SLC39A8
214719_at	9.64E-42	−2.44201	SLC46A3
203908_at	1.26E-54	−3.67051	SLC4A4
222155_s_at	7.00E-12	2.592536	SLC52A2
206874_s_at	4.76E-18	−2.3195	SLK
217707_x_at	1.12E-12	−2.39091	SMARCA2
219511_s_at	8.38E-28	−2.69503	SNCAIP
200869_at	3.98E-28	4.120789	RPL18A
213704_at	1.26E-20	−2.18703	RABGGTB
205573_s_at	2.33E-14	−2.15827	SNX7
218974_at	5.47E-12	−2.26683	SOBP
219993_at	1.06E-15	3.07392	SOX17
202936_s_at	5.41E-12	2.21883	SOX9
202363_at	4.65E-37	−3.20397	SPOCK1
218499_at	1.05E-39	−3.97485	STK26
212353_at	1.58E-07	−2.52873	SULF1
200911_s_at	2.89E-14	−2.55058	TACC1
205547_s_at	1.27E-05	2.423051	TAGLN
211276_at	4.89E-22	−4.06643	TCEAL2
204931_at	1.59E-13	−2.3008	TCF21
209277_at	4.74E-41	−3.06902	TFPI2
202085_at	1.98E-11	−2.06054	TJP2
204872_at	5.30E-16	−2.38261	TLE4
204427_s_at	4.47E-06	2.005576	TMED2
219895_at	5.40E-56	−3.32769	TMEM255A
201581_at	2.06E-17	−2.7922	TMX4
202704_at	7.51E-09	−2.14785	TOB1
203786_s_at	3.05E-19	−2.39369	TPD52L1
205803_s_at	1.24E-28	−2.47603	TRPC1
217979_at	2.13E-12	−2.34475	TSPAN13
203824_at	1.10E-07	−2.26876	TSPAN8
221493_at	2.73E-12	−2.1582	TSPYL1
202954_at	3.27E-13	2.116956	UBE2C
208998_at	4.92E-07	2.01738	UCP2
218449_at	3.47E-24	−2.37212	UFSP2
206658_at	5.85E-06	−2.15834	UPK3B

Supplementary Table 1. *Continued*

Probe ID	Adjusted p-value	logFC	Gene symbol
201568_at	2.24E-10	2.09715	UQCRQ
218396_at	4.06E-15	–2.05476	VPS13C
203892_at	7.53E-16	3.604279	WFDC2
206458_s_at	7.11E-42	–2.66765	WNT2B
213425_at	2.59E-32	–2.78657	WNT5A
201294_s_at	2.93E-28	–2.29403	WSB1
206067_s_at	1.66E-09	–2.10521	WT1
210996_s_at	1.47E-13	2.28527	YWHAE
213156_at	2.99E-15	–2.27837	ZBTB20
212982_at	1.24E-23	–2.2579	ZDHHC17
219778_at	4.63E-09	–2.75905	ZFPM2
209814_at	5.51E-27	–2.677	ZNF330
222028_at	5.81E-39	–2.07903	ZNF45
204175_at	7.25E-13	2.08818	ZNF593

Supplementary Table 2. DEGs that were significantly correlated with the overall survival of OC patients.

Gene Symbol	HR	LCI	UCI	p-value
IGF2	1.155904	1.077828	1.239634	4.90E-05
RECK	1.692166	1.308165	2.188887	6.19E-05
PTGER3	1.687189	1.293083	2.201411	1.16E-04
PHACTR2	1.648691	1.255291	2.16538	3.25E-04
PSD3	1.853413	1.305842	2.630593	5.53E-04
GPRASP1	1.374989	1.145661	1.65022	6.25E-04
PDGFD	1.335095	1.122146	1.588455	0.001115
ABCA8	1.244154	1.09064	1.419277	0.001149
PDE8B	1.850172	1.275062	2.684682	0.001198
DCN	1.216478	1.080111	1.37006	0.001236
ECM2	1.367841	1.128223	1.658349	0.001434
GFPT2	1.60216	1.196773	2.144866	0.001541
KDR	2.496187	1.38058	4.513284	0.002468
EFEMP1	1.259244	1.081612	1.46605	0.002967
CHGN	1.328542	1.095567	1.611061	0.00388
HOXC6	1.346405	1.09994	1.648096	0.003934
ALDH1A2	1.275981	1.079367	1.508409	0.00431
C6ORF111	1.426383	1.116916	1.821593	0.004426
ALDH1A1	1.227977	1.064256	1.416885	0.004909
CAV2	1.337283	1.091337	1.638657	0.005065
PDPN	1.512641	1.126845	2.030523	0.005871
MEF2C	1.422748	1.105835	1.830484	0.006099
LOC653754	1.658216	1.154323	2.38207	0.00621
RHOT1	1.568865	1.135197	2.168202	0.00637
LYPD1	0.836817	0.735941	0.951521	0.006564
RARRES1	1.157035	1.04117	1.285793	0.006741
NAP1L3	1.311493	1.074959	1.600075	0.007534
FLJ10159	1.295373	1.069451	1.569022	0.00813
SNCAIP	1.421542	1.092331	1.849971	0.00887
ADH1B	1.176641	1.041035	1.329911	0.009223
PEG3	1.124622	1.028839	1.229323	0.009711
BAMBI	1.275562	1.060642	1.534031	0.009728
CAV1	1.2066	1.046258	1.391516	0.009836
FZD7	1.266187	1.058346	1.514845	0.009885
ARHGAP6	1.40526	1.083322	1.822872	0.010382
NR2F2	1.211887	1.046241	1.40376	0.010384
OLFML1	1.322555	1.064904	1.642543	0.011446
IFI27	0.86593	0.773997	0.968784	0.011945
D4S234E	0.789259	0.656001	0.949586	0.012135
FLRT2	1.210822	1.040809	1.408606	0.013208
ADH1B	1.156958	1.030396	1.299065	0.013643
MTUS1	1.309358	1.056877	1.622154	0.013659
GALC	1.370127	1.06575	1.761433	0.014019
PPAP2A	1.361571	1.063615	1.742995	0.014309
NR2F1	1.222508	1.039093	1.438298	0.015421
RHOB	1.18208	1.028311	1.358843	0.018643
H2BFS	0.830951	0.710199	0.972233	0.020808
SLC39A4	0.818461	0.690484	0.970158	0.020933
GALNT12	0.685402	0.496802	0.9456	0.021413
RNASE4	1.212845	1.028974	1.429573	0.021422
SEMA3C	1.180876	1.024728	1.360817	0.021589
LAMA4	1.278289	1.03396	1.580354	0.023297
LOC283537	1.60001	1.064437	2.405058	0.023805
CIRBP	1.263725	1.028987	1.552012	0.025581
DOCK4	1.212601	1.022502	1.438043	0.026709
ADH5	1.245144	1.023108	1.515367	0.028674
LAMB1	1.212653	1.019134	1.442919	0.029733
MAF	1.301021	1.022468	1.655462	0.032297
ACSL1	1.220492	1.01449	1.468325	0.034645
IGFBP6	1.214964	1.01361	1.456317	0.035188
PURA	1.299578	1.016925	1.660796	0.036252
FGF13	1.436342	1.019623	2.023374	0.038348
TCF21	1.217575	1.009436	1.468631	0.039576
RARRES1	1.129291	1.002043	1.272699	0.046215

Supplementary Table 3. Characteristics of the 5 genes in the signature.

Gene symbol	Gene title	Coefficient
LYPD1	LY6/PLAUR domain containing 1	–0.02463
DCN	decorin	0.021033
RARRES1	retinoic acid receptor responder 1	0.033396
PEG3	paternally expressed 3	0.047122
IGF2	insulin like growth factor 2	0.105386